Available online at www.sciencedirect.com
ScienceDirect
Journal of Magnetic Resonance 188 (2007) 196–205
JMR Journal of Magnetic Resonance
www.elsevier.com/locate/jmr

A novel approach to the simulation of nitroxide spin label EPR spectra from a single truncated dynamical trajectory

V.S. Oganesyan

CMSB, Centre for Metalloprotein Spectroscopy and Biology, Henry Wellcome Unit of Biological EPR, School of Chemical Sciences and Pharmacy, University of East Anglia, Norwich NR4 7TJ, UK

Received 1 March 2007; revised 6 July 2007
Available online 17 July 2007

Abstract

A simple effective method for calculation of EPR spectra from a single truncated dynamical trajectory of spin probe orientations is reported. It is shown that an accurate simulation can be achieved from the small initial fraction of a dynamical trajectory until the point when the autocorrelation function of re-orientational motion of spin label has relaxed. This substantially reduces the amount of time for spectra simulation compared to previous approaches, which require multiple full length trajectories (normally of several microseconds) to achieve the desired resolution of EPR spectra. Our method is applicable to trajectories generated from both Brownian dynamics and molecular dynamics (MD) calculations. Simulations of EPR spectra from Brownian dynamical trajectories under a variety of motional conditions including bi-modal dynamics with different hopping rates between the modes are compared to those performed by conventional method. Since the relatively short timescales of spin label motions are realistically accessible by modern MD computational methods, our approach, for the first time, opens the prospect of the simulation of EPR spectra entirely from MD trajectories of real proteins structures.

Keywords: Computer simulation of EPR spectra; Electron paramagnetic resonance (EPR); Brownian dynamics trajectories; Molecular dynamics (MD)

1. Introduction

Multi-frequency electron paramagnetic resonance (EPR) with spin labels emerges as a particularly valuable advanced spectroscopic method for studying complex protein structure and dynamics with the advantage of being applicable to large proteins, to protein complexes in solution phase as well as in membranes and micelles and even on the surfaces of whole cells [1–6]. In proteins spin labels are introduced by genetic techniques with nitroxide probes attached to cysteine residues engineered into selected sites by directed mutagenesis. The nitroxide group which is positioned at the desired location on the protein serves as a reporter of local structure and dynamics [3,7].

By placing spin labels along a polypeptide chain a unique set of local structure data and protein chain dynamics is observed. EPR acts as a "snapshot" of very fast molecular motions and can resolve re-orientational dynamics of the attached spin label on a sub-nanosecond timescale. But EPR spectra are generally not easy to interpret and require full computer simulation. Considerable effort has been attempted in the past in developing a theoretical framework for the simulation of EPR lineshapes. Currently, there are two general theoretical approaches to the simulation of the EPR of spin labels undergoing motions with orientational constrains. First, the model developed by Freed and co-workers based on the stochastic Liouville approach [8,9]. The second, described by Robinson et al. [10], is based on the simulation of EPR spectra from Brownian rotational diffusion trajectories of spin-label orientations. The method by Freed and co-workers has been widely applied to study proteins, amorphous polymers and nucleic acids with remarkable success [1,11–13]. The advantage of this model is its relative ease of simulation and analysis when simple forms of ordering potential are considered. However, this method requires restoring

E-mail address: V.oganesyan@uea.ac.uk

1090-7807/$ - see front matter © 2007 Elsevier Inc. All rights reserved.
doi:10.1016/j.jmr.2007.07.001

potentials expressed analytically in terms of spherical harmonics with adjustable coefficients and becomes inadequate for complex potential energy surfaces. Most recently, Fajer et al. [14] have reported a method for calculating these coefficients from the probability distribution obtained from MD simulation. Although this approach provides all the information about tilt angles and ordering directly from MD calculations, varying coefficients within the uncertainty bounds obtained from the MD analysis was required to improve the fits. More importantly, the method depends on varying the principle diffusion tensor rates as adjustable parameters to fit EPR spectra. For such complex averaged potential energy surfaces, obtained from MD simulation the Brownian dynamics trajectories (DT) approach is more appropriate. Once the averaged potential surface is defined, the nitroxide can be approximated by a single particle exposed to a mean force, resulting from this potential. This approach, which is based on the numerical solution of Langevin equation, has been successfully used by Steinhoff and Hubbell for the simulation of X-band EPR spectra of a spin labelled poly-leucine α-helix trimer [15] and by White et al. to monitor changes in colicin protein complex [16].

Despite the enormous success, both stochastic Liouville and Brownian DTs approaches have several limitations: (i) they are based on approximate models of motion and cannot be routinely applied in general case; (ii) they rely on a number of parameters to describe motions, such as, rotational diffusion tensors of the spin label and protein domain and parameters which describe, or at least are needed to improve the description of motional constrains; and (iii) both methods require the fitting of adjustable parameters. Because of the large number of parameters involved, the solution need not be unique and may also be difficult to find. The situation is further complicated by the fact that, in general, the potential energy surface of the motions of a spin label tether and the surrounding protein atoms is a complicated function of space and cannot be easily described by a limited number of parameters.

For these reasons, it is important to develop a method so that the dynamics of spin labelled molecule under study could be modelled on a computer, and an EPR spectrum simulated directly. The importance of such a method has been recognised previously [17]. A MD trajectory generated by the modern molecular modelling techniques contains all the information necessary to calculate the EPR spectrum. Several examples of MD simulations for biomolecular systems with spin labels and probes have been reported in the literature. This include spin-labelled lipids [18], photosynthetic units [19], spin labelled T4L, myosin [17,20] and bacteriorhodopsin [21]. The simulations were carried out to extract EPR relevant information, such as the effective potential energy surfaces, rotational diffusion constants and order parameters. Simulation of EPR spectra require long dynamical trajectories to ensure a proper Fourier integration of the time-domain EPR signal [10,17,22]. MD trajectories generated by modern computers are still too short for this purpose. Only a few attempts have been made to use the results of MD calculations to simulate EPR spectra. The need for dynamical trajectories substantially longer than those attainable by MD calculations imposes a major challenge and requires additional theoretical modelling. Westlund and co-workers [18,23] have employed the extrapolation of free induction decay generated from MD trajectories using so-called ''flexible Brownian dynamics model'' while Stoica [20] used ''appended'' trajectory from short MD trajectories. The latter method requires the absence of high jumps in the vicinity of the points of appendage which is problematic.

In the present paper we formulate a so-called 'rapid' method for the accurate simulation of the EPR spectra from the small initial fraction of dynamical trajectory (DT) until the point when the auto-correlation function of re-orientational motion of spin label has relaxed. This approach is based on the fact that the time scale of the spin label motion is much shorter than the total sampling time. Experimental and computational studies on various labelled proteins indicate that diffusion motion of a spin label does not exceed the time scale of several nanoseconds [17,22,24,25]. For example, according to studies on the regulatory domain of scallop myosin [17], most trajectories of spin label orientations converge within 1 ns with potential energy and RMS differences remaining stable over longer periods of time (~6–10 ns). This research shows that the overall motion is a superposition of the fast motion contribution, when the label explores the conformations about a central dynamic mode of restriction (50 ps), and a slow motion, when the spin label samples different modes (~0.5 ns). Therefore, all the information required to simulate EPR spectra should be contained in the sampling trajectory on the much shorter timescale of the correlation time of the spin label orientations, the decay time of the autocorrelation function. These times can in fact be readily accessed by modern MD simulation methods. We have, therefore, developed a numerical procedure to extrapolate the rest of the time dependent magnetisation trajectories with high accuracy.

Our method is illustrated using DTs generated from the Brownian Dynamics diffusion model. Several types of spin label motion, both isotropic and restricted with different rotational diffusion correlation times, have been used to simulate EPR spectra and the results compared to those simulated by conventional algorithm using long DTs. Lastly, we discuss the application of this method to the case of multi-modal dynamics of spin label. The method reported in this paper opens for the first time the way for direct simulation of EPR spectra of proteins from a single MD trajectory.

2. Method

A general approach to direct EPR spectral simulation is first to generate a large number of trajectories of records of molecular and spin-label orientations [10]. These trajectories are then used in the equation for the spin density

matrix to define the time-dependent stochastic part of the spin-Hamiltonian at each particular discrete moment of time. Numerical solutions of this equation provide the time dependence for the transverse spin magnetisation for each particular initial orientation of the spin probe. The contributions to the CW EPR spectrum are then given by the Fourier transform of each magnetisation trajectory. Finally, the total line shape intensity is averaged over all possible initial orientations with the proper equilibrium distribution. The trajectories and magnetisation vectors are sampled N times at intervals Δt for a total time interval $T = N\Delta t$, where time resolution Δt is defined by the Nyquist criteria [26]. A typical EPR total spectral width of a nitroxide spin label, say, at X-band is about 80 G and at W-band is 155 G. To achieve the desired resolution of ~0.1 G between frequency points after Fourier transform a trajectory should be $T > 2$ μs [10]. To generate a reliable trajectory of such a length from MD simulations is computationally very demanding even for a moderate size molecule and, in the most cases, simply impossible. Therefore, it is not surprising that at the present there is no general method to simulate EPR spectra directly from a DT generated from molecular modelling.

Following Robinson et al. [10], the transverse magnetisation curve for each of the three hyperfine lines of a nitroxide spin label is calculated using the following integral form:

$$\langle M_+^m(t)\rangle = \langle M_+^m(0)\rangle \left\langle \exp\left(-\left[\mathrm{i}\int_0^t \omega^m(\tau)\,\mathrm{d}\tau + \frac{t}{T_2^m}\right]\right)\right\rangle \quad (1)$$

where $\langle\cdots\rangle$ indicates the ensemble average and the Larmor frequencies for the three hyperfine lines $\omega^m(t)$ are the functions of the orientation trajectory $\Omega(t)$ according to:

$$\begin{aligned}\omega^m(t) &= (g_{ZZ}(t)\beta B + A_{ZZ}(t)m)/\hbar\\ g_{ZZ}(t) &= g_{xx}l_{Zx}^2(\Omega(t)) + g_{yy}l_{Zy}^2(\Omega(t)) + g_{zz}l_{Zz}^2(\Omega(t))\\ A_{ZZ}(t) &= (C(h/\Delta A)\Delta A^2 l_{Zz}^2(\Omega(t))(l_{Zx}^2(\Omega(t)) + l_{Zy}^2(\Omega(t)))\\ &\quad + A_{xx}^2 l_{Zx}^2(\Omega(t)) + A_{yy}^2 l_{Zy}^2(\Omega(t)) + A_{zz}^2 l_{Zz}^2(\Omega(t)))^{1/2}\end{aligned} \quad (2)$$

B is the value of magnetic field, m is the projection of the nitrogen nuclear spin on its quantisation axis, which for ^{14}N is equal to ±1, 0. The principal values of the **g** and **A** tensors, respectively, are g_{ii}, A_{ii} with $\Delta A = A_{zz} - A_\perp$ and $l_{Zx}(\Omega(t)) = \sin\theta(t)\sin\phi(t)$, $l_{Zy}(\Omega(t)) = \sin\theta(t)\cos\phi(t)$, $l_{Zz}(\Omega(t)) = \cos\theta(t)$ denote the direction cosines between the nitroxide and laboratory axes which are the matrix elements of the transformation $\mathbf{L}(\Omega(t))$ that rotates the nitroxide axes into the laboratory axes [15] (see Fig. 1). The expressions for the resonance frequencies $\omega^m(t)$ are obtained using the high field approximation which assumes that hyperfine interaction is much less then the Zeeman one [15]. The time dependent fluctuations of $\omega^m(t)$ are caused by Brownian motion. In order to account for homogeneous line broadening of the EPR spectrum, the transverse relaxation time T_2^m is introduced. A special correlation function $C(t) = \langle l_{Zz}(\Omega(t))\cdot l_{Zz}(\Omega(0))\rangle$ in the equation for A_{ZZ} accounts for the time averaging of the pseudosecular terms in the spin-Hamiltonian due to re-orientational motion [15] where the value is taken at time $h/\Delta A$.

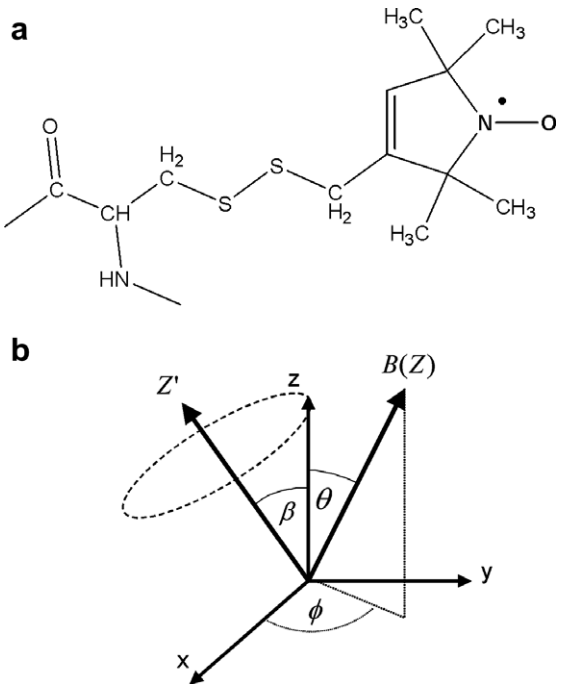

Fig. 1. Nitroxide spin label. (a) the molecular structure and (b) the orientation of the principal axes of magnetic tensors **g** and **A** relative to applied magnetic field (Z-axis of laboratory coordinate system) and to a vector of a mode of motion within the protein domain (Z'-axis of the protein fixed coordinate system). At each particular time the position of spin probe in the laboratory system is calculated using the product of two matrixes $\mathbf{L}''\cdot\mathbf{L}'(\Omega(t))$. $\mathbf{L}'(\Omega(t))$ transforms the nitroxide coordinate system into the protein fixed system and $\mathbf{L}''$ rotates the protein system into laboratory fixed coordinate system (see the text).

This DT approach, first introduced for fast motional limit [10] has later been improved by Steinhoff and Hubbell [15] by introducing non-secular terms into the calculation to cover the entire motional range. As will be shown later the improved version of Robinson's algorithm constitutes an appropriate base for the application of the method presented in this paper.

Our approach is based on the fact that the time dependence of the transverse magnetisation curve when the correlation function of the orientation of a spin probe has completely relaxed (~$10\tau_c$) is characterised by two parameters, namely, the stationary limit reached by the statistically averaged frequency of oscillation in the xy laboratory coordinate plane:

$$\bar{\omega}^m = \frac{1}{T}\int_0^T \langle\omega^m(\tau)\rangle\,\mathrm{d}\tau \quad (3)$$

and the relaxation rate of the averaged transverse magnetisation, λ^m.

The de-phasing of magnetisations is caused by the modulation of $\Delta\omega^m(t) = \omega^m(t) - \overline{\omega}^m$ due to the re-orientational

dynamics of the spin probe. T in (3) should be sufficiently long and for practical reasons the integral is taken over the period of time $T \geqslant 10\tau_c$ when the stationary limit has been reached.

For each hyperfine coupling line defined by the projection m of the nitrogen nuclear spin the actual value of the statistically averaged frequency depends on the initial orientation of a spin probe relative to a magnetic field and on the degree of constraints imposed on its motion.

Depending on the motional regime of spin label one should differentiate two cases.

2.1. Fast motional limit

In the fast motional limit $(\langle\Delta\omega(t)\Delta\omega\ (0)\rangle)^{-1/2} \gg \tau_c$, where τ_c is the correlation time of spin label motion, a Redfield approximation [27] can readily be used to calculate the relaxation rate. Fig. 2 illustrates the de-phasing of the averaged transverse magnetisation. Solid lines in Fig. 2a represent six magnetisation trajectories which eventually evolve out of phase from the same initial orientation. Circles in Fig. 2a show the magnetisation averaged over 500 Brownian DTs. This regime assumes that the motion is so fast that the de-phasing rate does not vary during the measurement interval. The de-phasing of magnetisation, caused by the modulation of the spin-Hamiltonian due to the re-orientational dynamics, can be accounted by time dependent perturbation theory [28]. According to the first-order perturbation theory the probability of transition in a time t for a single spin is given by:

$$W^m(t) = \frac{1}{2}\left|\int_0^t \Delta\omega^m(t')\,\mathrm{d}t'\right|^2 \tag{4}$$

Defining $t' - t'' = \tau$ this can be presented as:

$$\begin{aligned} W^m(t) &= \frac{1}{2}\int_0^t \mathrm{d}t' \int_0^t \Delta\omega^m(t')\Delta\omega^m(t'')\,\mathrm{d}t'' \\ &= \frac{1}{2}\int_0^t \mathrm{d}\tau \int_\tau^t \Delta\omega^m(t')\Delta\omega^m(t'-\tau)\,\mathrm{d}t' \\ &\quad + \frac{1}{2}\int_{-t}^0 \mathrm{d}\tau \int_0^{t+\tau} \Delta\omega^m(t')\Delta\omega^m(t'-\tau)\,\mathrm{d}t' \end{aligned} \tag{5}$$

The average $\langle W^m(t)\rangle$ should be taken on a stationary ensemble and therefore does not depend on the zero of time, in other words:

$$\langle\Delta\omega^m(t')\Delta\omega^m(t'-\tau)\rangle = \langle\Delta\omega^m(0)\Delta\omega^m(-\tau)\rangle = G^m(-\tau) \tag{6}$$

Eq. (6) defines the correlation functions $G^m(\tau)$ for $\Delta\,\omega^m(t)$.

Taking into account the fact that the classical equations of motion are reversible we have:

$$G^m(\tau) = G^m(-\tau) = \langle\Delta\omega^m(0)\Delta\omega^m(\tau)\rangle \tag{7}$$

After the averaging Eq. (5) reduces to the following form:

$$\langle W^m(t)\rangle = t\frac{1}{2}\int_{-t}^t G^m(\tau)\,\mathrm{d}\tau + \int_0^t \tau G^m(\tau)\,\mathrm{d}\tau \tag{8}$$

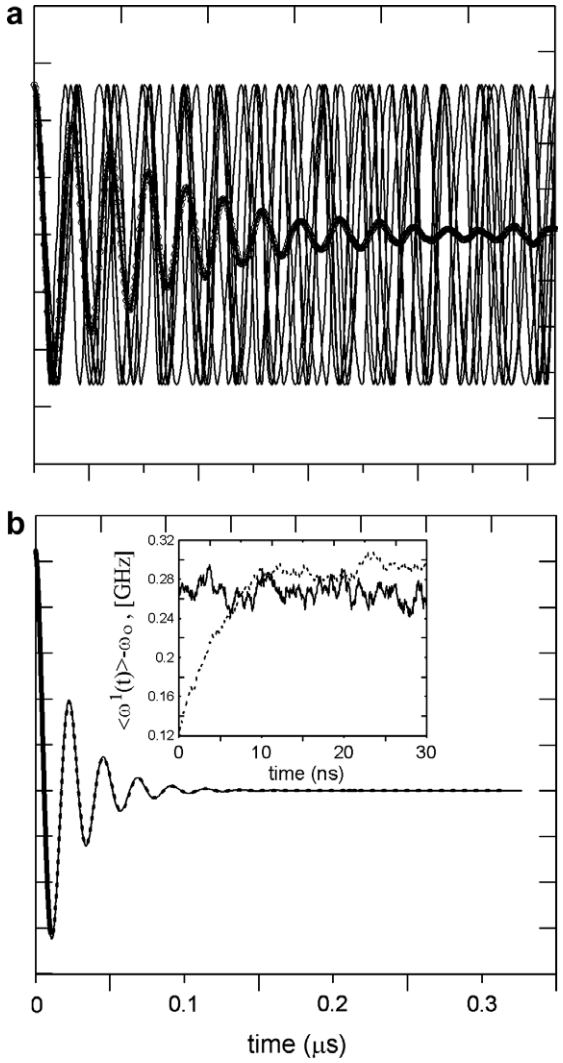

Fig. 2. (a) Evolution of 6 transverse magnetisation trajectories $M^1_{+i}(t)$ of the $m = 1$ hyperfine line for isotropic Brownian rotational diffusion of spin label orientations with $\tau_c = 1$ ns with the same initial orientation $z\|B$ (solid lines). Time evolutions are calculated in rotating frame. Magnetisation trajectory $\langle M^1_+(t)\rangle$ averaged over 500 full length Browniad DTs is shown by circles. (b) Comparison between averaged magnetization curve calculated by the conventional method using full length 500 DTs (dashed line) and by our new approach using single truncated DT of $20\tau_c$ in length (solid line). The bold solid line represents the averaged magnetization trajectory calculated numerically from the same truncated DT. Inset shows the time evolution of the averaged frequency $\langle\omega^1(t)\rangle$, solid line. Evolution of the averaged frequency, but for isotropic rotational diffusion with $\tau_c = 5$ ns (dashed line), is shown for comparison; ω_0 indicates microwave frequency of the X-band.

If $t \gg \tau_c$ the ratio of the two integrals in (8) is approximately t/τ_c, and the second one can be neglected compared with the first. A transition probability per unit time, the de-phasing rate, is defined as:

$$\lambda^m = \langle W^m(t)\rangle/t = J^m(0)/2 \tag{9}$$

where $J^m(0)$ is the spectral density at zero frequency given by the Fourier transform of the time correlation function:

$$J^m(\omega) = \int_{-\infty}^{\infty} G^m(\tau)\exp(-\mathrm{i}\omega\tau)\,\mathrm{d}\tau \tag{10}$$

In the latter expression the integration limits are replaced by $+\infty$ and $-\infty$. In practical terms, as in (3), the limits for numerical integration of (9) can be replaced by $\sim 10\tau_c$, the time when all $G^m(\tau)$ completely relax and the averaged frequencies $\langle\omega^m(t)\rangle$ reach their stationary limits. From this approximation one immediately realises that our method does not require the full length of DT to simulate the evolution of transverse magnetisations. An accurate simulation of the EPR spectra can be achieved from the small initial fraction of DT up to the point when the autocorrelation function of re-orientational motion of SL has relaxed ($\sim 10\tau_c$). The magnetisation trajectories can be predicted using (3) and (9). This is illustrated in Fig. 2b for an isotropic rotational diffusion of spin label with correlation time of 1 ns. The solid line represents the transverse magnetisation averaged over 500 DTs calculated for a total time interval of 0.4 microseconds. The dashed line is the prediction using Eqs. (3) and (9) and the truncated trajectory of ~10 ns in length. Additional relaxation observed in the Fig. 2b as compared to a pure de-phasing curve shown in Fig. 2a is due to homogeneous line broadening in the spectra described by T_2. Note, that in this particular case strong homogeneous broadening effectively reduces the sampling time T for DT, which is not generally the case. The difference between the two curves is scarcely distinguishable. The solid line in the inset shows the time evolution of the averaged resonance frequency which reaches stationary limit within 10 ns interval. Note an interesting fact associated with the stationary processes that the relaxation rate of transverse magnetisation, which describes the dynamics of the system out of equilibrium, can be evaluated from the properties of the system at equilibrium.

Generally, the correlation time is defined as: $\tau_c = \int_0^\infty \frac{C(t)}{C(0)}\,dt$ [22], where the zero-order correlation function $C(t)$ can be readily calculated from a Brownian or molecular DT. In a simple case when $G^m(\tau) = G^m(0)\exp(-|\tau|/\tau_c)$ the equation for the de-phasing rate reduces to a well known form [29]:

$$\lambda^m = \frac{\tau_c}{2}\langle|\omega^m(0) - \bar{\omega}^m|^2\rangle \tag{11}$$

At the opposite limit of completely restricted motion (the rigid limit) $\omega^m(t) - \bar{\omega}^m = 0$ for all times t and the motional contribution to relaxation is equal to zero, $\lambda^m = 0$.

In our approach the Cartesian matrix $\mathbf{L}'(\Omega(t))$ of spin label orientations in a protein coordinate system associated with the DT $\Omega(t)$ is calculated numerically over the period of time long enough to obtain reliable estimates for the correlation functions $G^m(\tau)$. The statistical average is computed with the "sliding time window" technique [22] with the overall length of the trajectory $T \sim (20\text{–}30)\tau_c$. Only one trajectory is generated. Finally to account for the random distribution of protein molecules relative to the magnetic field, a unitary transformation $\mathbf{L}''$ to a laboratory fixed system, whose Z-axis is defined along the applied magnetic field, is performed to obtain the direction cosines: $l_{Zi}(\Omega(t)) = \|\mathbf{L}'' \cdot \mathbf{L}'(\Omega(t))\|_{Zi}$. This calculation procedure is applied to each of the three ^{14}N hyperfine coupling lines contributing to EPR spectra. The contributions to the EPR absorption spectra are then given by the Fourier transform of each magnetisation trajectory. For the range of correlation times used in this paper ~900 points within the octant of a unit sphere were sufficient to simulate a spectrum with acceptable signal-to-noise level.

2.2. Slow motional limit

In the slow motional regime $(\langle\Delta\omega(t)\Delta\omega(0)\rangle)^{-1/2} \leqslant \tau_c$ the Redfield approximation is no longer valid. In other words, the autocorrelation functions $G^m(\tau)$ relax slowly during the time t of the measurement of transverse magnetisation $\langle M_+^m(t)\rangle$ and there are no reliable parameters to predict the behaviour of $\langle M_+^m(t)\rangle$ from the start. However, one can immediately realise that the very form of the evolution of transverse magnetisation (1) is formally an expression for a general de-phasing model with the phase being the time-integral over the fluctuating component of the energy difference [30]. After the correlation function for resonance frequency has completely relaxed the phase can be presented as a sum of two components:

$$\phi^m(t) = t\overline{\omega}^m(t') + \int_0^t \Delta\omega^m(t')\,dt' \tag{12}$$

Since $\lim_{t\to\infty}(\phi^m(t)/t) = \bar{\omega}^m$, $\lim_{t\to\infty}\left(\frac{1}{t}\int_0^t \Delta\omega^m(t')\,dt'\right) = 0$ and the fluctuating phase difference around the averaged frequency due to the stochastic motion of the spin label described by the second term in (12) has a finite variance and according to the central limit theorem [31] can be taken to be a Gaussian random variable, at least approximately [30]. For the Gaussian stationary process one can evaluate explicitly the average over the fluctuating phase factor using a known relation [32,33]:

$$\langle\exp(i\phi^m(t))\rangle = \exp\left(it\bar{\omega}^m(t) - \frac{1}{2}\langle\Delta\omega^m(t)^2\rangle\right) \tag{13}$$

where

$$\langle\Delta\omega^m(t)^2\rangle = \int_0^t dt' \int_0^t \langle\Delta\omega^m(t')\Delta\omega^m(t'')\rangle\,dt'' \tag{14}$$

For times $t > 10\tau_c$ we can approximate this as:

$$\langle\Delta\omega^m(t)^2\rangle = t\int_{-\infty}^{\infty}\langle\Delta\omega^m(0)\Delta\omega^m(\tau)\rangle\,d\tau = tJ^m(0) \tag{15}$$

which together with the statistically averaged frequency $\bar{\omega}^m$ are formally equivalent to the parameters describing the transverse magnetisation at the fast motional limit.

Therefore, we can draw an important conclusion, that at times when the autocorrelation function for the resonance frequency fluctuation has completely relaxed, the rest of the magnetisation can be approximated using two parameters, namely, $\bar{\omega}^m$ and λ^m of the stationary process under both motional regimes. This is illustrated by Fig. 2b, where

the bold solid line represents averaged magnetisation trajectory calculated numerically from a single DT for the time interval $0 \leqslant t \leqslant 10\tau_c$. The rest of it is predicted using (3) and (9).

2.3. General numerical procedure for EPR spectra simulation

Overall, the following computational procedure can be applied to cover both motional regimes.

1. A single dynamical trajectory is calculated for the $T \sim (20\text{–}30)\tau_c$ time interval long enough (normally between 1 ns and ~20 ns) to allow a statistical average of $\langle M_+^m(t)\rangle$ to be performed using a "sliding time window" technique. For this time interval the evolution of $\langle M_+^m(t)\rangle$ for each initial orientation $l_{zi}(\Omega(0))$ relative to magnetic field is calculated numerically using Eq. (1). The numerical counterpart of it is obtained using discrete times Δt giving the solution at each time step [10]:
$$\langle M_+^m(t+\Delta t)\rangle \approx \langle M_+^m(t)\rangle \exp(-(i\bar{\omega}^m + 1/T_2^m)\Delta t) \cdot \langle \exp(\Delta\omega^m(t)\Delta t)\rangle \quad (16)$$
2. Two parameters described by (3) and (9) are calculated from this single DT for each particular orientation relative to the magnetic field and are used to predict the rest of the appropriate transverse magnetisations.
3. Finally, the Fourier transform of each magnetisation trajectory provides the contribution to the EPR spectrum. The total lineshape intensity must be averaged over all possible orientations in solution.

In the next section we will demonstrate the results of the tests of this method using generated Brownian DTs with a range of motional conditions and compare the results with the spectra simulated by conventional computational approach. We will also address the issue multi-modal dynamics of spin label motion often observed in EPR spectra.

3. Applications using short single Brownian DTs

We have tested our approach by the simulation of X- and W-band EPR spectra using Brownian rotational dynamics model of spin label motion. Tests have been performed for the spin label undergoing different rotational diffusion regime from fast to slow. Different types of motion, namely, isotropic, restricted by ordering potential and more complex dynamics involving examples of fast and slow diffusion between two rotameric states have been modelled. The differences between EPR spectra simulated using statistically averaged full length Brownian DTs and using a single truncated DT are minimal.

Simulation of EPR spectra by the conventional method with full length Brownian DTs generated from the solution of Langevin equation has been described elsewhere [15,16]. In brief, we have combined the Brownian dynamics approach with the introduction of ordering potentials for restricted mobility which are expressed using spherical harmonics. The details of how the potential is described by spherical harmonics can be found elsewhere [8,14]. The DT of a restricted motion is generated by a numerical solution of the Langevin equation with associated systematic torques [15]. Analytical expressions for systematic torques have been derived and are included in our simulation program EPRSSP_DYN [16]. The dynamics is approximated by a particle undergoing a Brownian rotational motion exposed to the mean force of a restoring potential imposed by the protein. This type of motion is associated with an order parameter S, calculated from the dynamical trajectories generated according to:

$$S = 1/2(3\langle\cos\beta^2\rangle - 1) \quad (17)$$

where β is the angle between the z-axis of the spin label and the vector of the mode of the motion directed along the minima of a restricted potential in the protein domain (Fig. 1b). The average is taken over all dynamical trajectories and at all points of time along the trajectory until the rotational correlation function relaxes. The following principal values for magnetic parameters: $g_{xx} = 2.0073$, $g_{yy} = 2.0073$, $g_{zz} = 2.0025$; $A_{xx} = A_{yy} = 6$ G, $A_{zz} = 36$ G are used for all simulations.

In order to speed up the overall calculation, we have presented the Langevin equation in matrix form. This allows us to calculate points for a large number of trajectories for every initial orientation at the same time. At each particular time $(t + \Delta t)$ a normal distribution random number generator function is used to generate a matrix of random numbers with the number of rows and columns equal to the number of trajectories and initial orientations, respectively. This matrix is then used to calculate new orientations from orientations at time t. The contributions to the EPR absorption spectra are then given by the Fourier transform of each magnetisation trajectory and proper orientational averaging. For the range of correlation times used in this paper, 500 and 1000 Brownian trajectories for X- and W-band, respectively, and 900 points within the octant of a unit sphere were sufficient for simulations.

3.1. Fast motional regime

Fig. 3 shows comparison between X- and W-band EPR spectra simulated by a conventional method and those simulated from a single truncated Brownian DT using Eqs. (3) and (9) in the fast motional approximation. For each initial orientation of the spin probe relative to a magnetic field these two equations are applied to predict appropriate transverse magnetisation curve. Statistical averaging is performed using the technique of "sliding time window". Pairs of simulations (a and b) and (c and d) represent isotropic and restricted types of motions, respectively, with different correlation times for rotational diffusion. Orientational trajectories of the spin label used in the simulation of spectra (a and c) in Fig. 3 in which the directional cosine

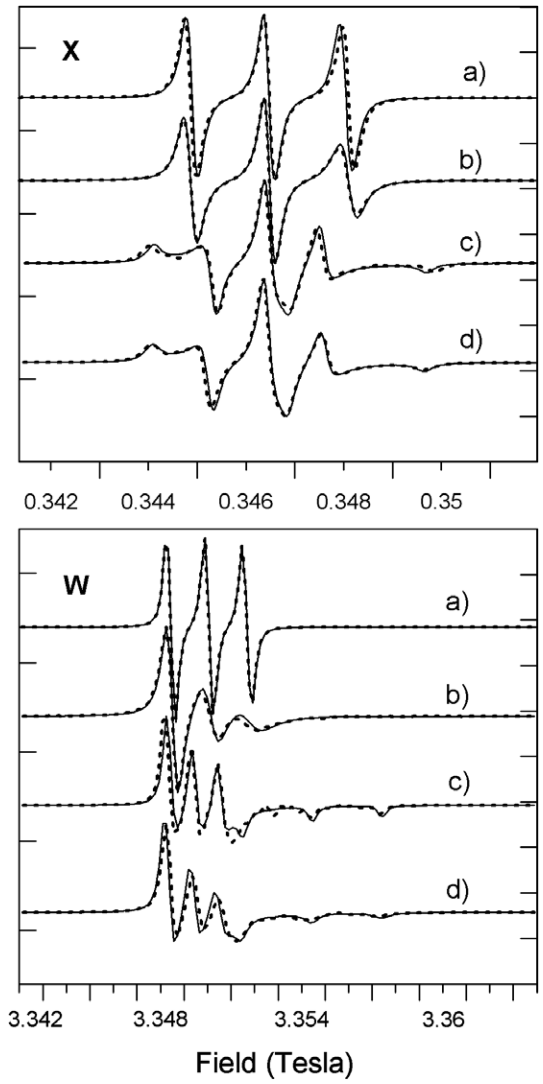

Fig. 3. Fast motional regime. Comparison between X- and W-band EPR spectra simulated with the method based on full length DTs (dashed lines) and the one based on the single truncated DT (solid lines). 500 DTs and 1000DTs are used with the conventional method in the simulation of X- and W-band spectra, respectively. (a) $\tau_c = 0.01$ ns, $S = 0$; (b) $\tau_c = 0.5$ ns, $S = 0$; (c) $\tau_c = 0.01$ ns, $S = 0.61$; and (d) $\tau_c = 0.5$ ns, $S = 0.58$.

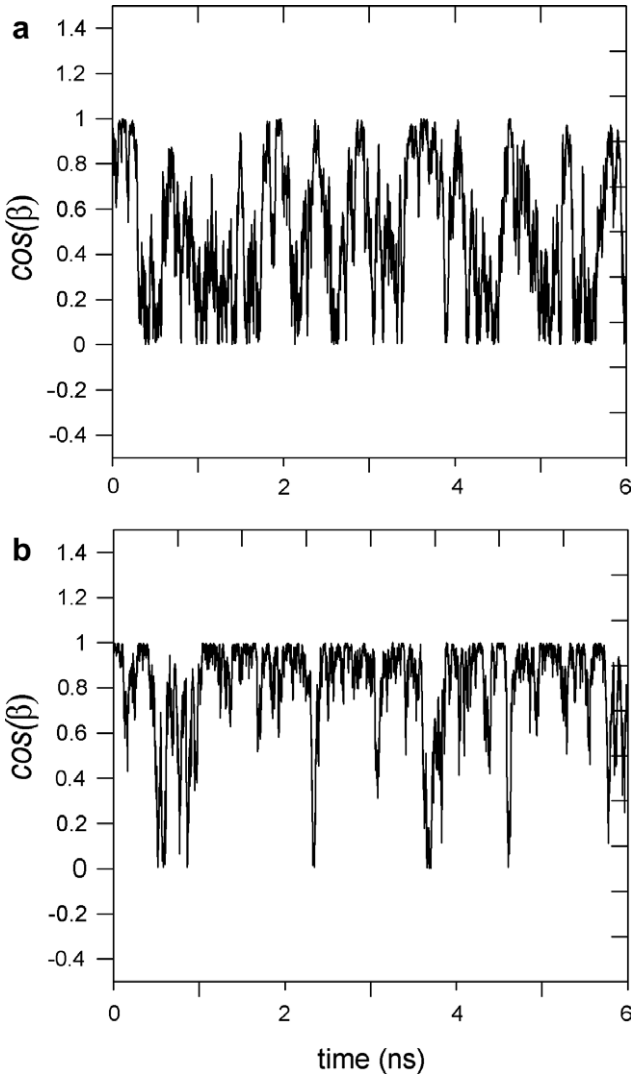

Fig. 4. Orientational trajectories of the spin label used in the simulation of EPR spectra by "rapid" method. Directional cosine $l'_{Zz}(\Omega(t))$ of spin label orientation is plotted over time. (a) $\tau_c = 0.01$ ns, $S = 0$; and (b) $\tau_c = 0.01$ ns, $S = 0.61$.

$l'_{Zz}(\Omega(t)) = \cos(\beta(t))$ is plotted over time are shown in Fig. 4 (a and b), respectively. All eight simulations demonstrate that for X- and W-bands the fast motional regime holds when $\tau_c \leqslant 1ns$ and the accurate simulation of EPR spectra can be achieved using (3) and (9) to predict magnetisation trajectories for the entire time range. For higher microwave frequencies the upper limit for correlation time should be scaled inversely.

3.2. Slow motional regime

Fig. 5 shows a comparison between the simulations of X- and W-band EPR spectra using the old conventional and the new methods in the slow motional regime. Spectra simulated by the conventional method with full length trajectories and by the procedure outlined in the previous section are shown in as curves solid (a) and dashed (a) curves, respectively. The solid curves (b) in each plot are obtained using Eqs. (3) and (9) applied over the entire time range of magnetisation curves. Clearly, the neglect of the numerical simulation of the initial fraction of magnetisation curve results in an inadequate simulation of spectra. In particular, both X and W-band simulations lack the high field features, which tend to be "averaged out". In addition, the position of the low field peak in the X-band simulation is shifted towards high field and the central features in the W-band spectrum are "smeared out". Both are artefact effects due to "inappropriate averaging". On the other hand, simulations performed from a single truncated DT with the numerical calculation of the evolution of magnetisation curves until the autocorrelation function of spin label motion has completely relaxed are almost indistinguishable from the "exact" simulations. In fact, the

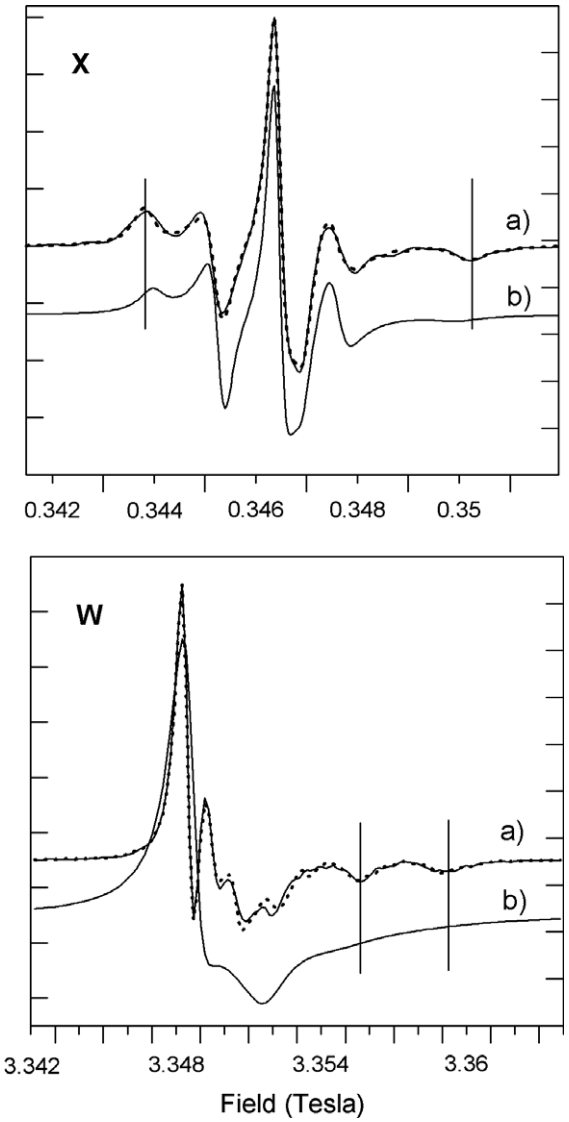

Fig. 5. Slow motional regime. Comparison between X- and W-band EPR spectra simulated by the method based on full length DTs (dashed lines – a), "rapid" method in the fast motional approximation (solid lines – b) and using "rapid" method with the proper numerical procedure for slow motions described in the text (solid lines – a). The number of trajectories used by conventional method are the same as in Fig. 4. $\tau_c = 5$ ns, $S = 0.58$.

simulation of the W-band spectrum from a single DT appears to be smoother than the one calculated using the ensemble of DTs. For W-band spectra a number of trajectories larger than 1000 is required to improve the quality of spectrum which will result in a substantial increase of computing time.

It is worth noting that because of the use of approximations one could assume that the speed in computation by the new method should be achieved at the expense of some accuracy. However, it is important to recognise that the old method is based on the numerical solution of Eq. (16) for the thransverse magnetisations for the full lengths of DTs while the new approach requires numerical integration only along the initial truncated part of the DT. This, in principle, can generate an accumulative error in the old method comparable to or even larger than the one associated with the approximations of the new method.

3.3. Bi-modal dynamics

In this section examples of more complex types of spin label dynamics are considered. Experimental EPR studies [16,34], MD simulations [17,20,22] and X-ray crystallography [35] on spin labelled proteins indicate that in many cases the spin probe trajectory can be approximated by so-called bi-modal dynamics. A common feature observed in the autocorrelation profiles obtained from MD simulations is that spin label exhibits a fast internal motion within the modes (~10–100 ps) and a slow diffusion between the modes (100 ps and 1 ns) [20,22]. The observation of two independent modes having two different correlation times and restrictions is not uncommon in spin label EPR and is usually seen where the motion of the side chain is partially restricted. This is less likely if the motion is either highly restricted or very mobile [16,34,35].

In order to describe multi-modal dynamics of spin label we have introduced into the Brownian DT program a so-called "hopping" model of the spin label [16]. This assumes an additional slow component in the motion due to transitions between localised modes described by forward and backward hopping rates between each pair of discrete rotameric states. In the case of only two modes of motion this model reduces to the two-jump problem described in [10]. For ordered, or non-evenly distributed, samples each "jump" between a pair of states would require a unitary transformation of the spin label orientation described by a rotational matrix connecting the dirtections of two modes of motion within a protein domain. For randomly oriented molecules this operation is not necessary since all possible orientations relative to magnetic field are taken into consideration at each particular time step. In order to generate the evolution in time associated with the "jumps" between different states the dynamic Monte Carlo simulation algorithm has been applied [36].

Fig. 6 illustrates the application of the new method for the simulation of EPR spectra for three different hopping rates between two modes of motion, namely isotropic and restricted along an axial potential with $S = 0.62$. Appropriate X-band spectra of individual modes are shown as curves (a and c) in the top panel of Fig. 3. In all simulations the forward and backward hopping rates are equal to each other. The solid line (a) in Fig. 6 shows the simulation with the rates $k_{\rightarrow}$ and $k_{\leftarrow}$, both on the scale of the rotational diffusion times. In this case the simulation is a complete average between two motions. As the hopping rate decreases some collapse of each hyperfine line is observed – Fig. 6b. In the situation when the hopping rates become sufficiently slow (10^7 s^{-1}) compared to the rotational correlation times, the overall EPR line shape manifests itself as the sum of independent contributions from two individual modes (Fig. 6c). In cases (a and b) the correlation time $k^{-1}_{\rightarrow(\leftarrow)}$ of the hopping component in the

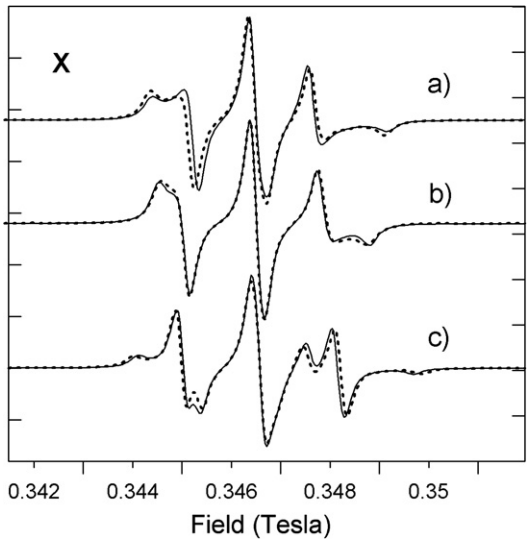

Fig. 6. Bi-modal dynamics. Comparison between X-band EPR spectra simulated by the method based on full length DTs (dashed lines) and the one based on the single truncated DT (solid lines). The number of trajectories used with the conventional method are the same as in Fig. 4. Individual modes are described by (a and c) of Fig. 4. The following values for hopping rates have been used in the simulations: (a) $k_{\rightarrow} = k_{\leftarrow} = 100 \times 10^9\ \mathrm{s}^{-1}$; (b) $k_{\rightarrow} = k_{\leftarrow} = 3 \times 10^9\ \mathrm{s}^{-1}$; and (c) $k_{\rightarrow} = k_{\leftarrow} = 0.01 \times 10^9\ \mathrm{s}^{-1}$.

overall motion is on the nanosecond timescale and the parameters (3) and (9) can be readily calculated from a single DT. However, in the case of (c) the overall DT becomes too long for practical application of the "rapid" method. The DT of such motion is shown in Fig. 7. Since jumps are rare ($k^{-1}_{\rightarrow(\leftarrow)} \gg 10\tau_c$; one for the entire time interval as seen in Fig. 7) the trajectory can be subdivided into the parts associated with each discrete mode of motion. This process can be assisted by considering the derivative $\partial \bar{l}'_{Zi}(t)/\partial t$ of the parameter $l'_{Zi}(\Omega(t))$ which is averaged over

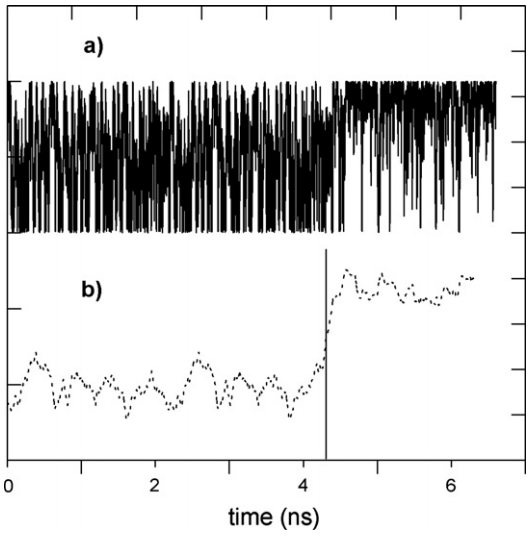

Fig. 7. Bi-modal DT with slow diffusion between two modes ($k_{\rightarrow} = k_{\leftarrow} = 0.01 \times 10^9\ \mathrm{s}^{-1}$). (a) Directional cosine $l'_{Z_2}(\Omega(t))$ of spin label orientation; and (b) $\bar{l}'_{Z_2}(\Omega(t))$ averaged over the intervals of 0.2 ns. Parameters for individual modes are given in Fig. 3a and c.

the intervals of $10\tau_c$ as shown in Fig. 7b. Sharp increases in the derivative would indicate the boundary points in the time domain. The method described in this paper can be applied to each of the sub-trajectories individually followed by carrying out additional averaging among sub-trajectories.

4. Conclusion

A simple and effective approach to the calculation of EPR spectra from a single truncated DT has been introduced. The method described requires only a small initial fraction of DT (normally up to several nanoseconds for most spin label motions) to achieve a desired resolution of EPR spectra. The method has been tested for different types of spin label motions using Brownian DTs. There are two major advantages of this method. Firstly, contrary to the other approaches which require the generation of multiple full length DTs, this method uses a single short DT. This reduces the amount of time for the simulation of EPR spectra substantially, by a factor of ~1000, as shown by our test simulations. This allows one to perform simulations of dynamical EPR spectra on a reasonable timescale using a common PC. Secondly, since these short timescales are realistically accessible by modern MD computational methods, our method can be applied to generate EPR spectra directly from MD trajectories of real protein structures. This ultimately opens the possibility of "computer engineering" of spin-labelled proteins with the desired properties prior to experiment. This should allow the prediction of sites for spin label attachment that will produce the required level of orientation and mobility to study a particular problem. The method can also be generalised to EPR spectra simulation for any type of spin radical. The application of this method in combination with MD simulations would allow, for the first time, simulation of EPR spectra entirely from MD trajectories of proteins. Such applications are currently in progress.

Acknowledgments

I thank the EPSRC for an Advanced Fellowship. Wellcome Trust is acknowledged for funding of the Henry Wellcome Unit for Biological EPR. Professor A.J. Thomson is gratefully acknowledged for reading the manuscript and for constructive comments and suggestions.

References

[1] P.P. Borbat, A.J. Costa-Filho, K.A. Earle, J.K. Moscicki, J.H. Freed, Electron spin resonance in studies of membranes and proteins, Science 291 (2001) 266–269.
[2] L.J. BerlinerSpin Labeling: The Next Millennium, Biological Magnetic Resonance, vol. 14, Plenum Press, NewYork, 1998.
[3] W.L. Hubbell, C. Altenbach, Investigation of structure and dynamics in membrane proteins using site-directed spin labelling, Curr. Opin. Struct. Biol. 4 (1994) 566–573.
[4] B.J. Gaffney, D. Marsh, High-frequency, spin-label EPR of nonaxial lipid ordering and motion in cholesterol-containing membranes, Proc. Natl. Acad. Sci. USA 95 (1998) 12940–12943.

[5] T. Prisner, M. Rohrer, F. MacMillan, Pulsed EPR spectroscopy: biological applications, Annu. Rev. Phys. Chem. 52 (2001) 279–313.
[6] J.H. Freed, New technologies in electron spin resonance, Annu. Rev. Phys. Chem. 51 (2000) 655–689.
[7] W.L. Hubbell, D.S. Cafiso, C. Altenbach, Identifying conformational changes with site-directed spin labelling, Nat. Struct. Biol. 7 (2000) 735–739.
[8] D.E. Budil, S. Lee, S. Saxena, J.H. Freed, Nonlinear-least-squares analysis of slow-motion EPR spectra in one and two dimensions using a modified Levenberg–Marquardt algorithm, J. Mag. Res. Ser. A 120 (1996) 155–189.
[9] L.J. Schwartz, A.E. Stillman, J.H. Freed, Analysis of electron spin echoes by spectral representation of the stochastic Liouville equation, J. Chem. Phys. 77 (1982) 5410–5425.
[10] B.H. Robinson, L.J. Slutsky, F.P. Auteri, Direct simulation of continuous wave electron paramagnetic resonance spectra from Brownian dynamics trajectories, J. Chem. Phys. 96 (1992) 2609–2616.
[11] J.P. Barnes, Z. Liang, H.S. Machaourab, J.H. Freed, W.L. Hubbell, A multifrequency electron spin resonance study of T4 Lysozyme dynamics, Biophys. J. 76 (1999) 3298–3306.
[12] M. Ge, J.H. Freed, Electron spin resonance study of aggregation of gramicidin in dipalmoylphosphatidylcholine bilayers and hydrophobic mismatch, Biophys. J. 76 (1999) 264–280.
[13] Z. Liang, J.H. Freed, R.S. Keyes, A.M. Borbat, An electron spin resonance model of DNA dynamics using the slowly relaxing local structure model, J. Phys. Chem. B 104 (2000) 5372–5381.
[14] D.E. Budil, K.L. Sale, K.A. Khairy, P.G. Fajer, Calculating slow-motional electron paramagnetic resonance spectra from molecular dynamics using a diffusion operator approach, J. Phys. Chem. A 110 (2006) 3703–3713.
[15] H.-J. Steinhoff, W.L. Hubbell, Calculation of electron paramagnetic resonance spectra from Brownian dynamics trajectories: application to nitroxide side chains in proteins, Biophys. J. 71 (1996) 2201–2212.
[16] G.F. White, L. Ottignon, T. Georghiou, C. Kleanthous, G.R. Moore, A.J. Thomson, V.S. Oganesyan, Analysis of nitroxide spin label motion in a protein–protein complex using multiple frequency EPR spectroscopy, J. Mag. Res. 185 (2007) 191–203.
[17] L.E.W. LaConte, V. Voelz, W. Nelson, M. Enz, D.D. Thomas, Molecular dynamics simulation of site-directed spin labeling: experimental validation in muscle fibers, Biophys. J. 83 (2002) 1854–1866.
[18] P. Hakansson, P.O. Westlund, E. Lindahl, O. Edholm, A direct simulation of EPR slow-motion spectra of spin labelled phospholipids in liquid crystalline bilayers based on a molecular dynamics simulation of the lipid dynamics, Phys. Chem. Chem. Phys. 3 (2001) 5311–5319.
[19] H. Levanon, K. Möbius, Advanced EPR spectroscopy on electron transfer processes in photosynthesis and biomimetic model systems, Annu. Rev. Biophys. Biomol. Struct. 26 (1997) 495–540.
[20] I. Stoica, Using molecular dynamics to simulate electron spin resonance spectra of T4 lysozyme, J. Phys. Chem. B 108 (2004) 1771–1782.
[21] C. Beier, H.-J. Steinhoff, A structure-based simulation approach for electron paramagnetic resonance spectra using molecular and stochastic dynamics simulations, Biophys. J. 91 (2006) 2647–2664.
[22] I. Stoica, Force field impact and spin-probe modeling in molecular dynamics simulations of spin-labeled T4 lysozyme, J. Mol. Model. 11 (2005) 210–225.
[23] N. Usova, L. Perssoni, P.O. Westlund, Theory of slow-motion EPR lineshapes for studies of membrane curvature, Phys. Chem. Chem. Phys. 2 (2000) 2785–2793.
[24] V.P. Timofeev, V.I. Tsetlin, Analysis of the mobility of protein side chains by spin label technique, Biophys. Struct. Mech. 10 (1983) 93–108.
[25] E.T.J. Van Den Bremer, A.H. Keeble, A.J.W.G. Visser, A. Van Hoek, C. Kleanthous, A.J.R. Heck, W. Jiskoot, Ligand-induced changes in the conformational dynamics of a bacterial cytotoxic endonuclease, Biochemistry 43 (2004) 4347–4355.
[26] A.B. Pippard, Response and Stability, Cambridge University Press, 1985, ISBN 0-521-31994-3.
[27] R. Kubo, K. Tomita, A general theory of magnetic resonance absorption, J. Phys. Soc. Jpn. 9 (1954) 888.
[28] L. Banci, I. Bertini, C. Luchinat, Nuclear and Electron Relaxation: The Magnetic Nucleus – Unpaired Electron Coupling In Solution, VCH Verlagsgesellschaft Gmbh, 1991.
[29] A. Abragham, R.V. Pound, Influence of electric and magnetic fields on angular correlations, Phys. Rev. 92 (1953) 953–962.
[30] A. Stern, Y. Aharonov, Y. Imry, Phase uncertainty and loss of interference: a general picture, Phys. Rev. A 41 (1990) 3436.
[31] H. Tijms, Understanding Probability: Chance Rules in Everyday Life, Cambridge University Press, Cambridge, 2004.
[32] N.D. Mermin, A short simple evaluation of expressions of the Debye–Waller form, J. Math. Phys. 7 (1966) 1038.
[33] J.v. Delft, H. Schoeller, Bosonization for beginners – refermionization for experts, Ann. Phys. 4 (1998) 225.
[34] J.P. Barnes, Z. Liang, H.S. Machaourab, J.H. Freed, W.L. Hubbell, A multifrequency electron spin resonance study of T4 lysozyme dynamics, Biophys. J. 76 (1999) 3298–3306.
[35] R. Langen, K.J. Oh, D. Cascio, W.L. Hubbell, Crystal structures of spin labelled T4 lysozyme mutants: implications for the interpretation of EPR spectra in terms of structure, Biochemistry 39 (2000) 8396–8405.
[36] K.A. Fichthorn, W.H. Weinberg, Theoretical foundation of dynamical Monte Carlo simulations, J. Chem. Phys. 95 (1991) 1090–1095.